

Holographic energy loss near critical temperature in an anisotropic background

Qi Zhou^{1,*} and Ben-Wei Zhang^{1,†}

¹*Key Laboratory of Quark & Lepton Physics (MOE) and Institute of Particle Physics,
Central China Normal University, Wuhan 430079, China*

(Dated: July 26, 2023)

We study the energy loss of a quark moving in a strongly coupled QGP under the influence of anisotropy. The heavy quark drag force, diffusion coefficient, and jet quenching parameter are calculated using the Einstein-Maxwell-dilaton model, where the anisotropic background is characterized by an arbitrary dynamical parameter A . Our findings indicate that as the anisotropic factor A increases, the drag force and jet quenching parameter both increase, while the diffusion coefficient decreases. Additionally, we observe that the energy loss becomes more significant when the quark moves perpendicular to the anisotropy direction in the transverse plane. The enhancement of the rescaled jet quenching parameters near critical temperature T_c , as well as drag forces for a fast-moving heavy quark is observed, which presents one of the typical features of QCD phase transition.

I. INTRODUCTION

The heavy-ion collisions (HICs) experiments at the Relativistic Heavy Ion Collider (RHIC) and the Large Hadron Collider (LHC) are believed to create almost the most perfect fluid Quark Gluon Plasma (QGP) [1–4]. This provides a novel window for studying the physics of Quantum Chromodynamics (QCD) at a strongly coupled regime. Since the properties of a strongly coupled system cannot be reliably calculated directly by perturbative techniques, one has to resort to some nonperturbative approaches to overcome the challenges.

The AdS/CFT correspondence, initially proposed by Maldacena in 1997, makes a conjecture that the large N_c limits of certain conformal field theories in d -dimensions can be described in terms of string theory on the product of $(d+1)$ -dimensional Anti-de Sitter space with a compact manifold [5–7]. Following the efforts of pioneers, the correspondence is introduced to handle problems in gauge theory at the strongly coupled scenario [8–10]. Especially, since the QCD is a multiple scales theory, finding a gravity dual to all scales of QCD is one of the essential aims of the AdS/CFT correspondence. Although the precise gravity dual to QCD is still unknown, the $\mathcal{N} = 4$ supersymmetric Yang-Mills (SYM) and QCD may share the same qualitative features at finite temperature, which means one could capture the physics of strong coupled QCD by deformed AdS_5 [11–13]. One of the significant achievements of AdS/CFT correspondence is the computation of the ratio of shear viscosity over to entropy density of the QGP, which is $1/4\pi$ [14], a simple universal value on the gravity side [15]. Besides, plenty of real-time dynamical quantities were computed on the weakly coupled gravity side with top-down [16–18] and bottom-up [19–21] holographic QCD models, such as hydrodynamic transport coefficients [22–26], energy loss of ener-

getic parton travelling through the QGP [27–31], transverse momentum broadening [32, 33], the thermal photon and di-lepton production rates [34–37] and so on [38–41].

The QGP created during the experiments in HICs, is believed to be anisotropic both in momentum and coordinate space for a short time [42]. Roughly speaking, the pressures of the QGP along the transverse direction may be larger than the pressure along the beam direction at a very earlier time, due to the rapid expansion along the beam direction. It is noticed that only the holographic QCD models with anisotropy succeeded in attempting to reproduce energy dependence of the total multiplicity of experiments in HICs [43–45]. With gauge gravity duality, the anisotropic geometries have been investigated to understand the properties of the QGP for a long time. The neutral spatial anisotropic black brane solution was found originally at zero temperature [46] and soon at nonzero temperature [47, 48]. Furthermore, many other interesting constructions to this anisotropic system have been developed from different groups [49–55]. Besides, the strong magnetic field also plays an important role in HICs and is also a source of anisotropy [56–59]. Most of the holographic work on anisotropic systems currently focuses on the systems with a magnetic field and the systems with spatial anisotropy, corresponding to the strong magnetic field created during HICs and the earlier time anisotropic phase of QGP produced in HICs. Although the anisotropy in such models may be different from the real QGP, it is expected that this kind of effort could help to reveal some intrinsic features of this plasma [60–66].

Further, to locate the critical point on (μ, T) -plane and probe the properties around the critical point, lots of efforts have been devoted by different groups based on isotropic Einstein-Maxwell-dilaton (EMD) models [67–72] and EMD models with magnetic fields where the anisotropy is introduced by an external field [73–76]. Recently, the authors of [77, 78] proposed a new version of the EMD model, where the anisotropy is introduced at one spatial direction in metric. As we mentioned before, the metric ansatz in this model can accurately reproduce the energy dependence of the total particle mul-

* qizhou@mails.ccn.u.edu.cn

† bwzhang@mail.ccn.u.edu.cn

tiplicity, which is one of our motivations for studying the energy loss near T_c within this system. It is illuminating to conduct an investigation on the energy loss of an energetic parton in the presence of anisotropy with this new anisotropic bottom-up QCD system. Since the EMD model is designed to mimic the QCD deconfinement phase transition, it is also of great interest to utilize this anisotropic EMD model to study the propagation of a quark around critical temperature T_c . With much attention having been attracted by the recent BES program in HICs, we hope our study can provide some insights into a better understanding of the real-time dynamical properties around QCD critical point.

This paper is organized as follows. In Sec. II, we briefly introduce the EMD model with the spatial anisotropic background [78]. In Sec. III we derive the drag force of heavy quark energy loss when passing through the QGP with the classic trailing string model. In Sec. IV we compute non-relativistic diffusion parameters by using Einstein relation together with the results of Sec. III. And the numerical results of jet quenching parameters are discussed in Sec. V. In the end, we present a short summary in Sec. VI.

II. THE EMD MODEL

The EMD system with anisotropy has been studied by the authors of [78]. In this section, we briefly review this anisotropic holographic model starting from the Einstein-dilaton-two-Maxwell action,

$$S = \int \frac{d^5x}{16\pi G_5} \sqrt{-g} \times \left[R - \frac{f_1(\phi)}{4} F_{(1)}^2 - \frac{f_2(\phi)}{4} F_{(2)}^2 - \frac{1}{2} \partial_\mu \phi \partial^\mu \phi - V(\phi) \right] \quad (1)$$

where $F_{(1)}$ and $F_{(2)}$ are the field strength tensors of the two $U(1)$ gauge fields introduced to provide for the chemical potential and the anisotropy respectively, ϕ is the dilaton field and $V(\phi)$ denotes the dilaton potential. And $f_1(\phi)$ and $f_2(\phi)$ are the gauge kinetic functions representing the coupling with the two $U(1)$ gauge fields respectively.

For a holographic description of the hot and dense anisotropic QGP, one possible version of the anisotropic metric ansatz is employed as

$$ds^2 = \frac{L^2 b(z)}{z^2} \times \left[-g(z) dt^2 + dx^2 + z^{2-\frac{2}{A}} (dy_1^2 + dy_2^2) + \frac{dz^2}{g(z)} \right] \quad (2)$$

where L gives the AdS -radius, $b(z) = e^{2A(z)}$ denotes the warp factor, $g(z)$ stands for the blackening function. Following [77, 79], the function $\mathcal{A} = -\ln(bz^2 + 1)$ is chosen for a light quark system, and the function

$f_1 = e^{-cz^2 - \mathcal{A}(z)} z^{-2+\frac{2}{A}}$ is determined to reproduce the Regge spectrum. Since there is rotational invariance in the $y_1 y_2$ -direction, we denote the x -axis as the direction of anisotropy.

The arbitrary dynamical parameter A measures the degree of anisotropy and Lorentz symmetry violation in $y_1 y_2$ -plane. A relativistic jet parton is focused on in our study, and we intend to introduce a slight break in symmetry by setting the value of A very close to unit. As in [78], the authors found that continually increasing the value of A had a dramatic impact on the thermal properties of the system. Therefore we chose to constrain our calculations at zero chemical potential using slight anisotropy cases with A values of 1.01, 1.02, and 1.03 for convenience.

In the following calculations, we set the AdS radius L to be one for convenience. The solution for the blackening function may be obtained in

$$g(z) = 1 - \frac{\int_0^z (1 + b\xi^2)^{3a} \xi^{1+\frac{2}{A}} d\xi}{\int_0^{z_h} (1 + b\xi^2)^{3a} \xi^{1+\frac{2}{A}} d\xi} + \frac{2\mu^2 c}{L^2 (1 - e^{cz_h^2})^2} \int_0^z e^{c\xi^2} (1 + b\xi^2)^{3a} \xi^{1+\frac{2}{A}} d\xi \times \left[1 - \frac{\int_0^z (1 + b\xi^2)^{3a} \xi^{1+\frac{2}{A}} d\xi}{\int_0^{z_h} (1 + b\xi^2)^{3a} \xi^{1+\frac{2}{A}} d\xi} \frac{\int_0^{z_h} e^{c\xi^2} (1 + b\xi^2)^{3a} \xi^{1+\frac{2}{A}} d\xi}{\int_0^z e^{c\xi^2} (1 + b\xi^2)^{3a} \xi^{1+\frac{2}{A}} d\xi} \right]. \quad (3)$$

Calculating the derivative of the blackening function, the temperature is parameterized by z_h ,

$$T = \frac{|g'(z)|}{4\pi} \Big|_{z=z_h} = \frac{1}{4\pi} \left| -\frac{(1 + bz_h^2)^{3a} z_h^{1+\frac{2}{A}}}{\int_0^{z_h} (1 + b\xi^2)^{3a} \xi^{1+\frac{2}{A}} d\xi} \left[1 - \frac{2\mu^2 c e^{2cz_h^2}}{L^2 (1 - e^{cz_h^2})^2} \times \left(1 - e^{-cz_h^2} \frac{\int_0^{z_h} e^{c\xi^2} (1 + b\xi^2)^{3a} \xi^{1+\frac{2}{A}} d\xi}{\int_0^{z_h} (1 + b\xi^2)^{3a} \xi^{1+\frac{2}{A}} d\xi} \right) \times \int_0^{z_h} (1 + b\xi^2)^{3a} \xi^{1+\frac{2}{A}} d\xi \right] \right|, \quad (4)$$

where z_h denotes the location of the horizon.

And the dilaton field $\phi(z)$ reads

$$\phi(z) = \int_{z_0}^z d\xi \times \frac{2\sqrt{A-1} + [2(A-1) + 9aA^2] b\xi^2 + K}{(1 + b\xi^2) A\xi} \quad (5)$$

and

$$K = [A - 1 + 3a(1 + 2a)A^2] b^2 \xi^4. \quad (6)$$

There are no divergences in the isotropic case $A = 1$ for the dilaton field, but in the anisotropic cases, the dilaton field has a logarithmic divergence with $\phi(z) \approx \frac{2\sqrt{A-1}}{A} \text{Log}(\frac{z}{z_h})$. It is proposed in [78, 80] that a sufficiently small boundary condition point z_0 should reproduce the proper behavior of the scalar field. In this paper,

we take $a = 4.046$, $b = 0.01613$, $c = 0.227$ to be compatible with results in the isotropic case [79], where the critical temperature is around $T_c = 157.8$ MeV.

III. DRAG FORCE

In small momentum transfer limit, the multiple scattering of heavy quarks with thermal partons in the QGP can be treated as Brownian motion [81, 82], which can be described by the Langevin equation as,

$$\frac{dp}{dt} = -\eta_{DP} + f_{drive}. \quad (7)$$

When the heavy quark moves with a constant velocity v , the driving force f_{drive} is equal to the drag force $f_{drag} = \eta_{DP}$.

In gauge theory side, the heavy quark suffers a drag force and consequently loses its energy while traveling through the strongly coupled plasma. On gravity side, this process could be modeled by a trailing string [27, 28], and the drag force f_{SYM} in isotropic SYM plasma with zero chemical potential is then given by

$$f_{SYM} = -\frac{\pi T^2 \sqrt{\lambda}}{2} \frac{v}{\sqrt{1-v^2}}, \quad (8)$$

where $\sqrt{\lambda} = \frac{L^2}{\alpha'} = \sqrt{g_{YM} N_c}$. The energy loss of the heavy quark can be understood as the energy flow from the endpoint along the string towards the horizon of the world sheet.

We follow the argument in [27, 28] to analyze the energy loss of a heavy quark in the anisotropic background. The drag forces are calculated near the critical temperature T_c , and the string dynamics are captured by the Nambu-Goto string world-sheet action

$$S = -\frac{1}{2\pi\alpha'} \int d\tau d\sigma \sqrt{-\det g_{\alpha\beta}}, \quad (9)$$

$$g_{\alpha\beta} = \frac{\partial X^\mu}{\partial \sigma^\alpha} \frac{\partial X^\nu}{\partial \sigma^\beta}. \quad (10)$$

where $g_{\alpha\beta}$ is the induced metric, and $g_{\mu\nu}$ and X_μ are the brane metric and target space coordinates.

The trailing string corresponding to a quark moving on the boundary along the chosen direction $x_p (x_p = x, y_1, y_2)$ with a constant velocity v has the usual parametrization

$$t = \tau, x_p = vt + \xi(z), z = \tau. \quad (11)$$

Plugging static gauge Eq. (11) into the metric Eq. (2),

we have

$$ds^2 = g_{tt} dt^2 + g_{xx} dx_p^2 + g_{zz} dz^2, \quad (12)$$

$$g_{tt} = \frac{-L^2 b(z) g(z)}{z^2}, \quad (13)$$

$$g_{xx} = \frac{L^2 b(z)}{z^2 g(z)} \Big|_{(x_p=x)}, \quad (14)$$

$$g_{xx} = \frac{L^2 b(z) (z^{2-\frac{2}{A}})}{z^2 g(z)} \Big|_{(x_p=y_1, y_2)}, \quad (15)$$

$$g_{zz} = \frac{L^2 b(z)}{z^2 g(z)}. \quad (16)$$

The Lagrangian density can be obtained from the Nambu-Goto action as

$$\mathcal{L} = \sqrt{-g_{tt} g_{zz} - g_{zz} g_{xx} v^2 - g_{tt} g_{xx} \xi'^2} \quad (17)$$

The Lagrangian density does not depend on ξ from Eq. (17), which implies that the canonical momentum is conserved,

$$\Pi_\xi = \frac{\partial \mathcal{L}}{\partial \xi'} = \frac{-g_{tt} g_{xx} \xi'}{\sqrt{-g_{tt} g_{zz} - g_{zz} g_{xx} v^2 - g_{tt} g_{xx} \xi'^2}} \quad (18)$$

Then one can get

$$\xi^2 = \frac{-g_{zz} (g_{tt} + g_{xx} v^2) \Pi_\xi^2}{g_{tt} g_{xx} (g_{tt} g_{xx} + \Pi_\xi^2)} \quad (19)$$

Both the numerator and the denominator must change sign at the same location z from Eq. (19). The critical point z_c can be written as

$$g_{tt}(z_c) = -g_{xx}(z_c) v^2, \quad (20)$$

and

$$\Pi_\xi^2 = -g_{tt}(z_c) g_{xx}(z_c). \quad (21)$$

Finally, we obtain the drag force

$$f = -\frac{1}{2\pi\alpha'} \Pi_\xi = -\frac{1}{2\pi\alpha'} g_{xx}(z_c) v. \quad (22)$$

There are two different drag forces, $f^{v\parallel A}$ and $f^{v\perp A}$, for the anisotropy in background metric in Eq. (2). To be specific, $f^{v\parallel A}$ stands for the drag force in parallel with the anisotropy direction, when the jet parton moves along the anisotropy direction. And $f^{v\perp A}$ denotes the drag force in parallel with its motion direction when the jet parton moving perpendicular to the anisotropy direction. Plugging Eq. (12) into Eq. (22), we have

$$f^{v\parallel A} = -\frac{1}{2\pi\alpha'} g_{xx}(z_c) v \Big|_{x_p=x} \quad (23)$$

$$= -\frac{v}{2\pi\alpha'} \frac{b(z_c)}{z_c^2}, \quad (24)$$

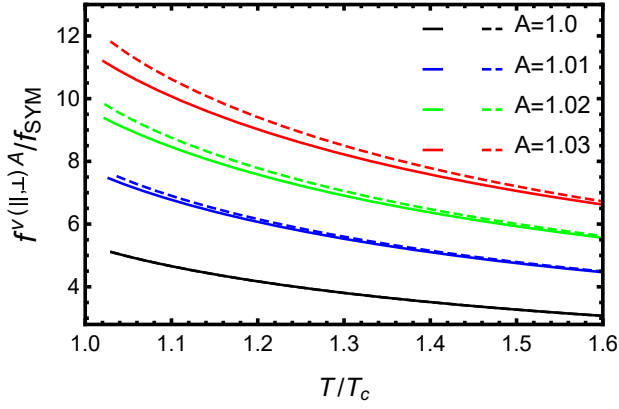


FIG. 1. Perpendicular (dashed line) and parallel (solid line) drag force at lower speed ($v = 0.6$) normalized by conformal limit as a function of the temperature for different values of the anisotropy factor A .

and

$$f^{v\perp A} = -\frac{1}{2\pi\alpha'} g_{xx}(z_c) v|_{x_p=y_1} \quad (25)$$

$$= -\frac{v}{2\pi\alpha'} b(z_c) z_c^{-\frac{2}{A}}. \quad (26)$$

The influence of spatial anisotropy on drag forces is illustrated in Fig. 1 and Fig. 2, where the drag forces in anisotropic plasma are rescaled by the isotropic SYM result at zero chemical potential given in Eq. (8). Fig. 1 shows, at lower speed ($v = 0.6$) the drag force $f^{v\parallel A}$ always becomes larger with increasing anisotropic factor A . A similar trend is also observed for drag forces perpendicular to anisotropy direction $f^{v\perp A}$. It is seen that the perpendicular direction drag force $f^{v\perp A}$ is larger than the parallel direction drag force $f^{v\parallel A}$ with the same anisotropic factor around critical temperature T_c .

At higher speed $v = 0.96$, corresponding to a faster charm quark, the situation becomes more complicated as presented in Fig. 2. Plots (a), (b), (c), and (d) in Fig. 2 present drag forces at different anisotropy $A = 1$, $A = 1.01$, $A = 1.02$ and $A = 1.03$ respectively. We find the drag force $f^{v\parallel A}$ always goes up with increasing anisotropic factor A . The perpendicular direction drag force $f^{v\perp A}$ is larger than the parallel direction drag force $f^{v\parallel A}$ around T_c . Furthermore, there is a peak near critical temperature T_c when the velocity of quark ($v = 0.96$) is approaching the speed of light. The enhancement of energy loss around critical temperature T_c is one of the typical features of QCD phase transition. From Fig. 1 and Fig. 2, we also find that the charm quark (with faster velocity and lighter mass) is more sensitive to properties of the anisotropy QGP than the bottom quark (with slower velocity and heavier mass) when they pass through the anisotropic plasma with a fixed initial energy E_i .

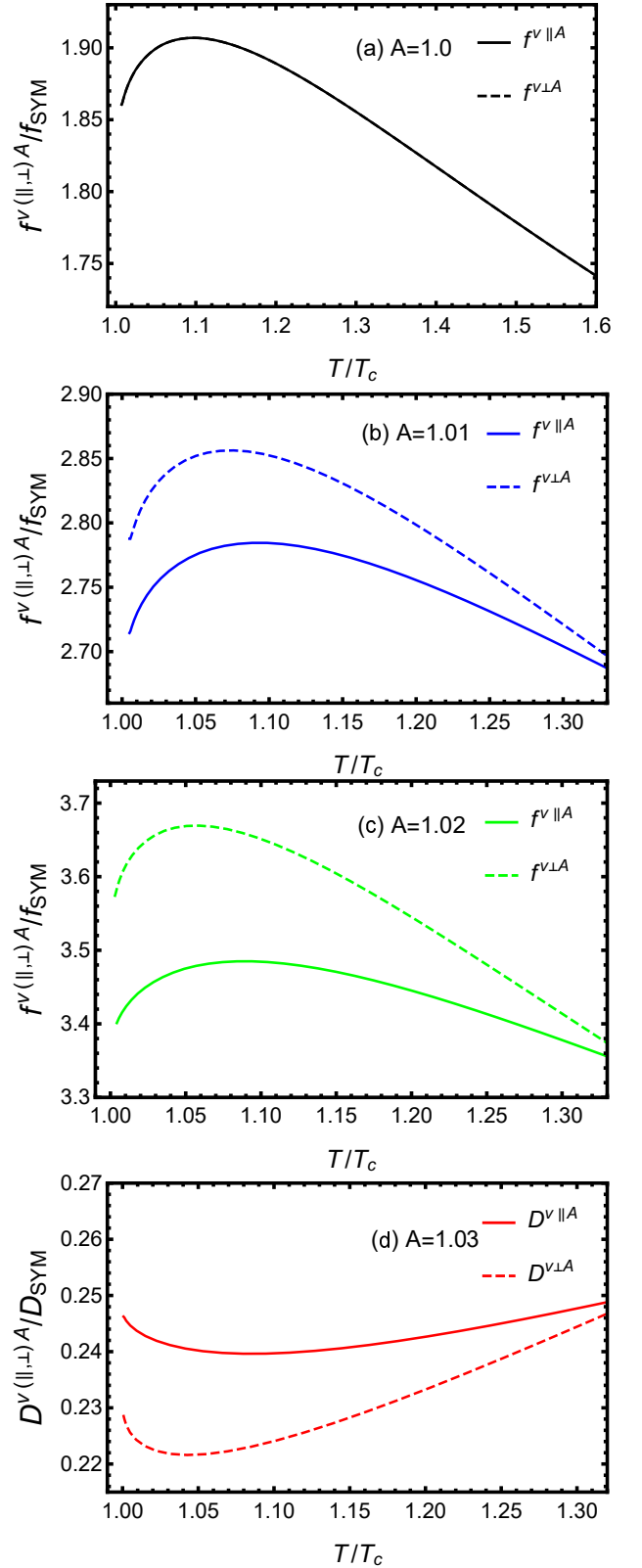


FIG. 2. Perpendicular (dashed line) and parallel (solid line) drag force at higher speed ($v = 0.96$) normalized by conformal limit as a function of the temperature for different values of the anisotropy factor A .

IV. DIFFUSION COEFFICIENT

The diffusion coefficient, another important transport parameter of plasma, has been studied extensively at the RHIC and the LHC. It is of a general practice to utilize the Einstein-Maxwell system to study this transverse momentum broadening when heavy quark propagation in plasma [83, 84]. The heavy quark transverse momentum diffusion constant D in the strongly coupled $\mathcal{N} = 4$ supersymmetric Yang-Mills theory was first computed in [32, 33], and then it was generalized to non-conformal theories in [85]. The Langevin dynamics of non-relativistic heavy quarks are completely determined by the momentum broadening D . The Einstein relation together with the expression of η_D allows us to infer the value of D for this strongly coupled anisotropic plasma. The diffusion coefficient in the isotropic SYM theory [33] is

$$D_{SYM} = \frac{T}{m} t_{SYM} = \frac{2}{\pi T \sqrt{\lambda}}, \quad (27)$$

where $t_{SYM} = \frac{1}{\eta_D}$ is the diffusion time.

From Eq. (22) and Eq. (27), we obtain diffusion coefficient in anisotropic plasma normalized by isotropic SYM results as,

$$\frac{D}{D_{SYM}} = \frac{\pi^2 T^2}{g_{xx}(z_c) \sqrt{1-v^2}} \Big|_{(x_p=x, y_1, y_2)}. \quad (28)$$

Now there are also two different diffusion coefficients, $D^{v\parallel A}$ and $D^{v\perp A}$, for the anisotropy in background metric Eq. (2). $D^{v\parallel A}$ gives the diffusion coefficient when jet partons move along anisotropy direction, while $D^{v\perp A}$ gives the one when the jet parton moves perpendicular to anisotropy direction. Plugging Eq. (12) into Eq. (28), we have

$$\frac{D^{v\parallel A}}{D_{SYM}} = \frac{\pi^2 T^2}{g_{xx}(z_c) \sqrt{1-v^2}} \Big|_{(x_p=x)} \quad (29)$$

$$= \frac{\pi^2 T^2}{b(z_c) z_c^{-2} \sqrt{1-v^2}} \quad (30)$$

and

$$\frac{D^{v\perp A}}{D_{SYM}} = \frac{\pi^2 T^2}{g_{xx}(z_c) \sqrt{1-v^2}} \Big|_{(x_p=y_1)} \quad (31)$$

$$= \frac{\pi^2 T^2}{b(z_c) z_c^{-\frac{2}{A}} \sqrt{1-v^2}}. \quad (32)$$

The numerical results of the influences on diffusion constants D from anisotropy factor are displayed in Fig. 3 and Fig. 4, normalized by the isotropic SYM result at zero baryon density given in Eq. (27). It is seen from Fig. 3 that, at lower speed ($v = 0.6$) both $D^{v\parallel A}$ and $D^{v\perp A}$ suffer stronger suppression with increasing anisotropic factor A . In addition, the perpendicular direction diffusion constant $D^{v\perp A}$ has stronger suppression

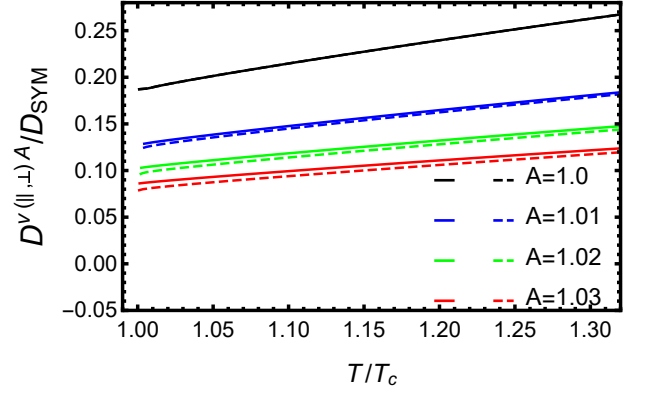


FIG. 3. Perpendicular (dashed line) and parallel (solid line) diffusion constants at lower speed ($v = 0.6$) normalized by conformal limit as a function of the temperature for different values of the anisotropy factor A .

than parallel direction diffusion constant $D^{v\parallel A}$ around critical temperature T_c .

Fig. 4 gives the results at a higher speed ($v = 0.96$), and plots (a), (b), (c), and (d) in Fig. 4 present diffusion constants at different anisotropy $A = 1$, $A = 1.01$, $A = 1.02$ and $A = 1.03$ respectively. We find diffusion constant $D^{v\parallel A}$ goes down with increasing anisotropic factor A . It is also seen that the perpendicular direction diffusion constant $D^{v\perp A}$ has stronger suppression than parallel direction diffusion constant $D^{v\parallel A}$ around critical temperature T_c . One may observe the strongest suppression near critical temperature T_c when the quark moves almost with the speed of light ($v = 0.96$). All numerical results show the same trend that the energy loss in the perpendicular direction is larger than the one in the parallel direction.

V. JET TRANSPORT PARAMETER

In dual gravity theory, a non-perturbative definition of jet transport coefficient \hat{q} has been provided [30], based on the computation of light-like adjoint Wilson loops for $\mathcal{N} = 4$ SYM plasma. It has been shown that the jet quenching parameter at an isotropic SYM plasma with zero chemical potential is

$$\hat{q}_{SYM} = \frac{\pi^{\frac{3}{2}} \sqrt{\lambda} T^3 \Gamma(\frac{4}{3})}{\Gamma(\frac{5}{4})}. \quad (33)$$

In this section, we discuss the jet quenching parameter \hat{q} in the anisotropic background. We follow the argument in [30, 86] to study the jet quenching parameter of a light quark system in an anisotropic medium, in which the jet quenching parameter \hat{q} is directly related to light-like adjoint Wilson loop [30] as

$$\langle W^A[C] \rangle \approx \exp \left[-\frac{1}{4\sqrt{2}} \hat{q} L^2 L^- \right], \quad (34)$$

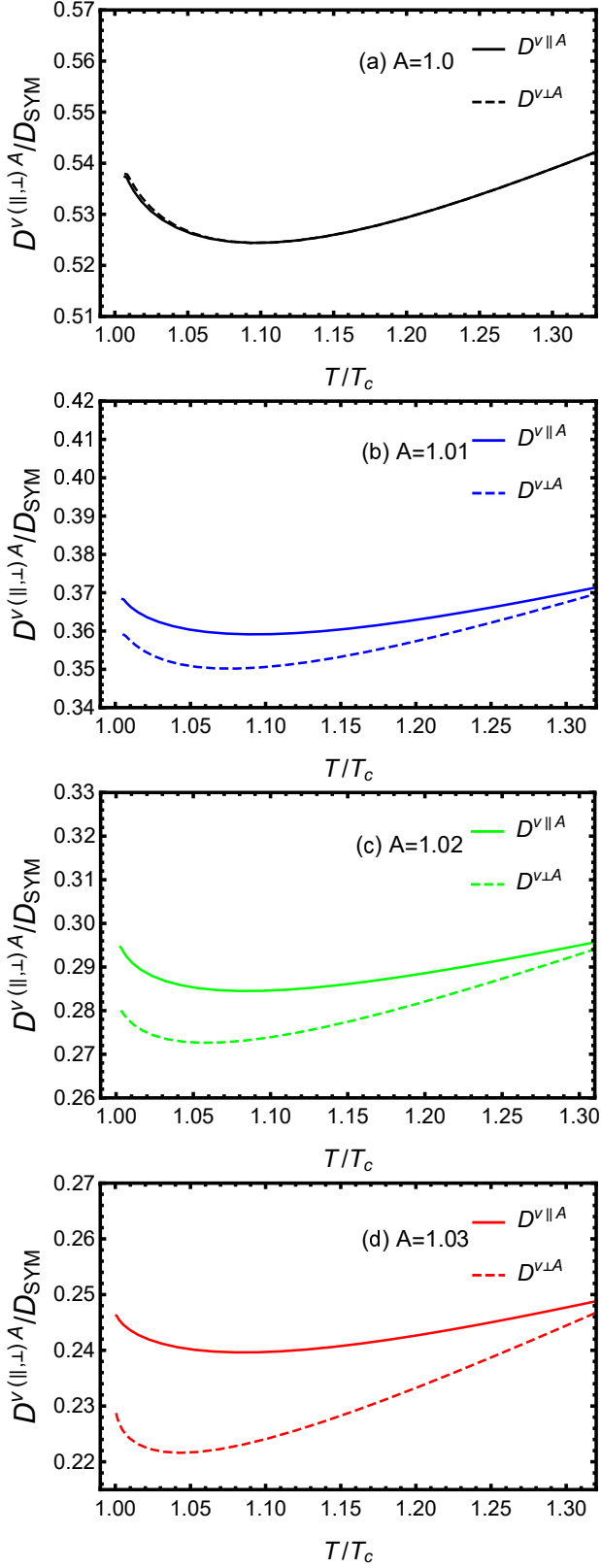


FIG. 4. Perpendicular (dashed line) and parallel (solid line) diffusion constants at higher speed ($v = 0.96$) normalized by conformal limit as a function of the temperature for different values of the anisotropy factor A .

where \mathcal{C} is a null-like rectangular Wilson loop formed by a quark-antiquark pair, L gives the separated distance, and L^- is the traveling distance along light-cone time duration.

Using the equations

$$\langle W^A[\mathcal{C}] \rangle \approx \langle W^F[\mathcal{C}] \rangle^2 \quad (35)$$

and

$$\langle W^F[\mathcal{C}] \rangle \approx \exp[-S_I], \quad (36)$$

we obtain a general relation of jet quenching parameter

$$\hat{q} = 8\sqrt{2} \frac{S_I}{L^- L^2}. \quad (37)$$

To calculate the Wilson loop, we take advantage of the light-cone coordinates

$$x_+ = \frac{t + x_p}{\sqrt{2}}, \quad x_- = \frac{t - x_p}{\sqrt{2}}, \quad (38)$$

where x_p is chosen to be the direction of motion.

The metric Eq. (2) is then given by

$$ds^2 = G_{--}(dx_+^2 + dx_-^2) + G_{+-}dx_+dx_- \quad (39)$$

$$+ G_{ii}dx_i^2 + G_{zz}dz^2, \quad (40)$$

$$G_{--} = \frac{g_{tt} + g_{pp}}{2}, \quad (41)$$

$$G_{+-} = \frac{g_{tt} - g_{pp}}{2}, \quad (42)$$

$$G_{ii} = g_{ii}|_{(i=x,y_1,y_2)}, \quad (43)$$

$$G_{zz} = g_{zz}. \quad (44)$$

Given the Wilson loop extending along the x_k direction, we choose static gauge coordinates

$$x_- = \tau, x_k = \sigma, u = u(\sigma). \quad (45)$$

The Nambu-Goto action Eq. (9) can be given as

$$S = \frac{L_-}{\pi\alpha'} \int_0^{\frac{L_k}{2}} d\sigma \sqrt{G_{--}(G_{zz}z'^2 + G_{kk})}. \quad (46)$$

As action Eq. (46) does not depend explicitly on σ explicitly, we could have a conserved quantity E

$$\frac{\partial \mathcal{L}}{\partial \dot{z}} \dot{z} - \mathcal{L} = E, \quad (47)$$

resulting in

$$\dot{z}^2 = \frac{(G_{kk}G_{--} - c^2)G_{kk}}{c^2G_{zz}}. \quad (48)$$

Combining Eq. (48) and Eq. (46), we get

$$S_0 = \frac{L_-}{\pi\alpha'} \int_0^{z_h} dz \sqrt{G_{uu}G_{--}}. \quad (49)$$

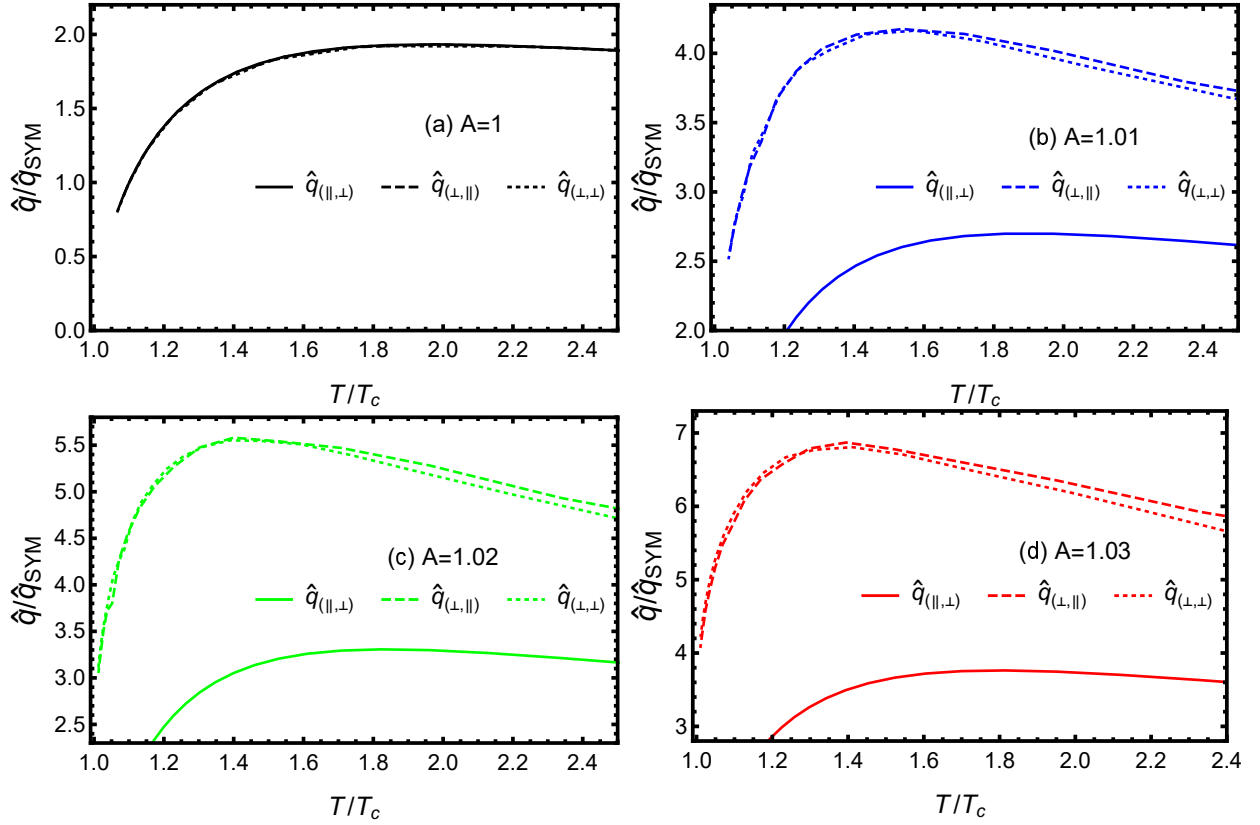


FIG. 5. Motion parallel to anisotropy (solid line) and perpendicular to anisotropy (dashed and dotted line) jet quenching parameter normalized by conformal limit as a function of the temperature for different values of the anisotropy factor A .

The total action is divergent and should be subtracted by the self-energy of the two free quarks part

$$S - S_0 = \frac{L_-}{\pi\alpha'} \int_0^{z_h} dz \sqrt{G_{zz}G_{--}} \left(\sqrt{\frac{G_{--}G_{kk}}{G_{--}G_{kk} - E^2}} - 1 \right) \quad (50)$$

In our calculation, indices p and k here denote a chosen direction. Substituting Eq. (50) into Eq. (37), we show

$$\begin{aligned} \hat{q}_{(p,k)} &= \frac{\sqrt{2}}{\pi\alpha'} \left(\int_0^{z_h} dz \frac{1}{G_{kk}} \sqrt{\frac{G_{zz}}{G_{--}}} \right)^{-1} \\ &= \frac{\sqrt{2}}{\pi\alpha'} \left(\int_0^{z_h} dz \frac{1}{g_{kk}} \sqrt{\frac{2g_{zz}}{g_{tt} + g_{pp}}} \right)^{-1} \end{aligned} \quad (51)$$

Now we see there are three types of jet quenching parameters, $\hat{q}_{(\parallel,\perp)}$, $\hat{q}_{(\perp,\parallel)}$ and $\hat{q}_{(\perp,\perp)}$ for anisotropic background given in Eq. (2). Here $\hat{q}_{(\parallel,\perp)}$ denotes the jet transport coefficient when energetic partons move along the anisotropy direction, and the momentum broadens perpendicular to anisotropy direction; $\hat{q}_{(\perp,\parallel)}$ stands for the jet quenching parameter when energetic partons move perpendicular to the anisotropy direction, and the momentum broadening along anisotropy; $\hat{q}_{(\perp,\perp)}$ gives the coefficient with fast parton moving perpendicular to anisotropy direction, and the momentum broadening per-

pendicular to anisotropy direction.

$$\begin{aligned} \hat{q}_{(\parallel,\perp)} &= \frac{\sqrt{2}}{\pi\alpha'} \left(\int_0^{z_h} dz \frac{1}{g_{y_1 y_1}} \sqrt{\frac{2g_{zz}}{g_{tt} + g_{xx}}} \right)^{-1} \\ &= \frac{\sqrt{2}}{\pi\alpha'} \left[\int_0^{z_h} dz \left(b(z) z^{\frac{2}{A}} \sqrt{\frac{2}{g(z)(-f(z) + 1)}} \right) \right]^{-1} \end{aligned} \quad (52)$$

$$\begin{aligned} \hat{q}_{(\perp,\parallel)} &= \frac{\sqrt{2}}{\pi\alpha'} \left(\int_0^{z_h} dz \frac{1}{g_{xx}} \sqrt{\frac{2g_{zz}}{g_{tt} + g_{y_1 y_1}}} \right)^{-1} \\ &= \frac{\sqrt{2}}{\pi\alpha'} \left[\int_0^{z_h} dz \left(b(z) z^{-2} \sqrt{\frac{2}{g(z)(-f(z) + z^{2-\frac{2}{A}})}} \right) \right]^{-1} \end{aligned} \quad (53)$$

$$\begin{aligned} \hat{q}_{(\perp,\perp)} &= \frac{\sqrt{2}}{\pi\alpha'} \left(\int_0^{z_h} dz \frac{1}{g_{y_1 y_1}} \sqrt{\frac{2g_{zz}}{g_{tt} + g_{y_1 y_1}}} \right)^{-1} \\ &= \frac{\sqrt{2}}{\pi\alpha'} \left[\int_0^{z_h} dz \left(b(z) z^{\frac{2}{A}} \sqrt{\frac{2}{g(z)(-f(z) + z^{2-\frac{2}{A}})}} \right) \right]^{-1} \end{aligned} \quad (54)$$

Fig. 5 demonstrates the impact of spatial anisotropy on jet quenching parameters, normalized by the isotropic SYM result at zero baryon density given in Eq. (33). Plots (a), (b), (c), and (d) in Fig. 5 show jet quenching parameters at different anisotropy $A = 1$, $A = 1.01$, $A = 1.02$ and $A = 1.03$ respectively. Figure (a) with $A = 1$ corresponds to the isotropic case. One see that all three jet quenching parameters $\hat{q}_{(\parallel,\perp)}$, $\hat{q}_{(\perp,\parallel)}$ and $\hat{q}_{(\perp,\perp)}$ increase with anisotropic factor A . And we observe the small peak around critical temperature T_c , which is one of the typical features of QCD phase transition. One reads from different anisotropic cases in Figures (b), (c), and (d) of Fig. 5, that in general $\hat{q}_{(\perp,\parallel)} \geq \hat{q}_{(\perp,\perp)} \geq \hat{q}_{(\parallel,\perp)}$, which indicates that the energy loss is larger in the transverse plane than along the anisotropic direction. It also shows that the momentum broadening of an energetic parton in the anisotropic medium depends more on the direction of motion rather than the direction of momentum broadening.

VI. CONCLUSION

The study of jet quenching properties as functions of parameters such as temperature, chemical potential, and anisotropy factor is of great relevance for understanding the anisotropic QGP. In the present work, we have taken the investigation on energy loss of a jet parton near T_c at zero chemical potential under the influence of anisotropy with an EMD model.

We focus on the influences of anisotropy on several im-

portant quantities related to parton energy loss near T_c . It is demonstrated that with increasing anisotropic factor A , the drag force and jet quenching parameter go up, while the diffusion constant goes down. The comparison of drag forces in different directions shows that energy loss near T_c is larger when moving perpendicular to the anisotropy direction than parallel to the anisotropy direction. The jet quenching parameter and diffusion constant also give the same conclusion that energy loss is stronger when the jet parton moves perpendicular to the anisotropy direction.

We also observe a peak near critical temperature T_c both on the drag force ($f^{v\parallel A}$ and $f^{v\perp A}$) and the jet quenching parameter ($\hat{q}_{(\perp,\parallel)}$, $\hat{q}_{(\perp,\perp)}$, and $\hat{q}_{(\parallel,\perp)}$) when energetic partons move nearly with the speed of light. However, when parton moves at a lower speed the peak of the drag force ($f^{v\parallel A}$ and $f^{v\perp A}$) near T_c may disappear. Moreover, comparing numerical results of the drag force at different speeds, we see charm quark is more sensitive to the properties of the plasma than the bottom quark when the initial jet energy is fixed.

ACKNOWLEDGMENTS

We thank Zhou-Run Zhu for his enlightening advice and very useful discussions. We also thank Zi-Qiang Zhang for his suggestions. This research is supported by the Guangdong Major Project of Basic and Applied Basic Research No. 2020B0301030008, and Natural Science Foundation of China with Project Nos. 11935007.

-
- [1] I. Arsene et al. Quark gluon plasma and color glass condensate at RHIC? The Perspective from the BRAHMS experiment. *Nucl. Phys. A*, 757:1–27, 2005.
 - [2] K. Adcox et al. Formation of dense partonic matter in relativistic nucleus-nucleus collisions at RHIC: Experimental evaluation by the PHENIX collaboration. *Nucl. Phys. A*, 757:184–283, 2005.
 - [3] B. B. Back et al. The PHOBOS perspective on discoveries at RHIC. *Nucl. Phys. A*, 757:28–101, 2005.
 - [4] John Adams et al. Experimental and theoretical challenges in the search for the quark gluon plasma: The STAR Collaboration’s critical assessment of the evidence from RHIC collisions. *Nucl. Phys. A*, 757:102–183, 2005.
 - [5] Juan Martin Maldacena. The Large N limit of superconformal field theories and supergravity. *Adv. Theor. Math. Phys.*, 2:231–252, 1998.
 - [6] Edward Witten. Anti-de Sitter space and holography. *Adv. Theor. Math. Phys.*, 2:253–291, 1998.
 - [7] S. S. Gubser, Igor R. Klebanov, and Alexander M. Polyakov. Gauge theory correlators from noncritical string theory. *Phys. Lett. B*, 428:105–114, 1998.
 - [8] Edward Witten. Anti-de Sitter space, thermal phase transition, and confinement in gauge theories. *Adv. Theor. Math. Phys.*, 2:505–532, 1998.
 - [9] Ofer Aharony, Steven S. Gubser, Juan Martin Maldacena, Hirosi Ooguri, and Yaron Oz. Large N field theories, string theory and gravity. *Phys. Rept.*, 323:183–386, 2000.
 - [10] Jorge Casalderrey-Solana, Hong Liu, David Mateos, Krishna Rajagopal, and Urs Achim Wiedemann. *Gauge/String Duality, Hot QCD and Heavy Ion Collisions*. Cambridge University Press, 2014.
 - [11] Joshua Erlich. How Well Does AdS/QCD Describe QCD? *Int. J. Mod. Phys. A*, 25:411–421, 2010.
 - [12] Amanda W. Peet and Joseph Polchinski. UV / IR relations in AdS dynamics. *Phys. Rev. D*, 59:065011, 1999.
 - [13] Umut Gursoy, Elias Kiritsis, Liuba Mazzanti, Georgios Michalogiorgakis, and Francesco Nitti. Improved Holographic QCD. *Lect. Notes Phys.*, 828:79–146, 2011.
 - [14] G. Policastro, Dan T. Son, and Andrei O. Starinets. The Shear viscosity of strongly coupled N=4 supersymmetric Yang-Mills plasma. *Phys. Rev. Lett.*, 87:081601, 2001.
 - [15] Alex Buchel and James T. Liu. Universality of the shear viscosity in supergravity. *Phys. Rev. Lett.*, 93:090602, 2004.
 - [16] Joseph Polchinski and Matthew J. Strassler. The String dual of a confining four-dimensional gauge theory. 3 2000.
 - [17] Andreas Karch and Emanuel Katz. Adding flavor to AdS / CFT. *JHEP*, 06:043, 2002.

- [18] Tadakatsu Sakai and Shigeki Sugimoto. Low energy hadron physics in holographic QCD. *Prog. Theor. Phys.*, 113:843–882, 2005.
- [19] Steven S. Gubser and Abhinav Nellore. Mimicking the QCD equation of state with a dual black hole. *Phys. Rev. D*, 78:086007, 2008.
- [20] U. Gursoy and E. Kiritsis. Exploring improved holographic theories for QCD: Part I. *JHEP*, 02:032, 2008.
- [21] B. Galow, E. Megias, J. Nian, and H. J. Pirner. Phenomenology of AdS/QCD and Its Gravity Dual. *Nucl. Phys. B*, 834:330–362, 2010.
- [22] Christopher P. Herzog. The Hydrodynamics of M theory. *JHEP*, 12:026, 2002.
- [23] Paolo Benincasa and Alex Buchel. Hydrodynamics of Sakai-Sugimoto model in the quenched approximation. *Phys. Lett. B*, 640:108–115, 2006.
- [24] Rudolf Baier, Paul Romatschke, Dam Thanh Son, Andrei O. Starinets, and Mikhail A. Stephanov. Relativistic viscous hydrodynamics, conformal invariance, and holography. *JHEP*, 04:100, 2008.
- [25] Javier Mas and Javier Tarrio. Hydrodynamics from the Dp-brane. *JHEP*, 05:036, 2007.
- [26] Makoto Natsuume and Takashi Okamura. Causal hydrodynamics of gauge theory plasmas from AdS/CFT duality. *Phys. Rev. D*, 77:066014, 2008. [Erratum: *Phys. Rev. D* 78, 089902 (2008)].
- [27] C. P. Herzog, A. Karch, P. Kovtun, C. Kozcaz, and L. G. Yaffe. Energy loss of a heavy quark moving through N=4 supersymmetric Yang-Mills plasma. *JHEP*, 07:013, 2006.
- [28] Steven S. Gubser. Drag force in AdS/CFT. *Phys. Rev. D*, 74:126005, 2006.
- [29] Andrej Ficnar, Steven S. Gubser, and Miklos Gyulassy. Shooting String Holography of Jet Quenching at RHIC and LHC. *Phys. Lett. B*, 738:464–471, 2014.
- [30] Hong Liu, Krishna Rajagopal, and Urs Achim Wiedemann. Calculating the jet quenching parameter from AdS/CFT. *Phys. Rev. Lett.*, 97:182301, 2006.
- [31] Kazem Bitaghsir Fadafan and Razieh Morad. Jets in a strongly coupled anisotropic plasma. *Eur. Phys. J. C*, 78(1):16, 2018.
- [32] Jorge Casalderrey-Solana and Derek Teaney. Transverse Momentum Broadening of a Fast Quark in a N=4 Yang Mills Plasma. *JHEP*, 04:039, 2007.
- [33] Steven S. Gubser. Momentum fluctuations of heavy quarks in the gauge-string duality. *Nucl. Phys. B*, 790:175–199, 2008.
- [34] Simon Caron-Huot, Pavel Kovtun, Guy D. Moore, Andrei Starinets, and Laurence G. Yaffe. Photon and dilepton production in supersymmetric Yang-Mills plasma. *JHEP*, 12:015, 2006.
- [35] Yan Yan Bu. Photoproduction and conductivity in dense holographic qcd. *Phys. Rev. D*, 86:026003, Jul 2012.
- [36] Shang-Yu Wu and Di-Lun Yang. Holographic Photon Production with Magnetic Field in Anisotropic Plasmas. *JHEP*, 08:032, 2013.
- [37] Leonardo Patino and Diego Trancanelli. Thermal photon production in a strongly coupled anisotropic plasma. *JHEP*, 02:154, 2013.
- [38] Zhou-Run Zhu, De-fu Hou, and Xun Chen. Potential analysis of holographic Schwinger effect in the magnetized background. *Eur. Phys. J. C*, 80(6):550, 2020.
- [39] Krishna Rajagopal, Andrey V. Sadofyev, and Wilke van der Schee. Evolution of the jet opening angle distribution in holographic plasma. *Phys. Rev. Lett.*, 116(21):211603, 2016.
- [40] Zhou-Run Zhu, Jun Chen, and Defu Hou. Gravitational waves from holographic QCD phase transition with gluon condensate. *Eur. Phys. J. A*, 58(6):104, 2022.
- [41] Jing Zhou, Jun Chen, Le Zhang, Jialun Ping, and Xun Chen. Holographic Schwinger Effect in Anisotropic Media. 1 2021.
- [42] Michael Strickland. Thermalization and isotropization in heavy-ion collisions. *Pramana*, 84(5):671–684, 2015.
- [43] Elias Kiritsis and Anastasios Taliotis. Multiplicities from black-hole formation in heavy-ion collisions. *JHEP*, 04:065, 2012.
- [44] I. Ya. Aref’eva, E. O. Pozdeeva, and T. O. Pozdeeva. Holographic estimation of multiplicity and membranes collision in modified spaces AdS_5 . *Theor. Math. Phys.*, 176:861–872, 2013.
- [45] Irina Ya. Aref’eva and Anastasia A. Golubtsova. Shock waves in Lifshitz-like spacetimes. *JHEP*, 04:011, 2015.
- [46] Tatsuo Azeyanagi, Wei Li, and Tadashi Takayanagi. On String Theory Duals of Lifshitz-like Fixed Points. *JHEP*, 06:084, 2009.
- [47] David Mateos and Diego Trancanelli. Thermodynamics and Instabilities of a Strongly Coupled Anisotropic Plasma. *JHEP*, 07:054, 2011.
- [48] David Mateos and Diego Trancanelli. The anisotropic N=4 super Yang-Mills plasma and its instabilities. *Phys. Rev. Lett.*, 107:101601, 2011.
- [49] Long Cheng, Xian-Hui Ge, and Sang-Jin Sin. Anisotropic plasma at finite $U(1)$ chemical potential. *JHEP*, 07:083, 2014.
- [50] Long Cheng, Xian-Hui Ge, and Sang-Jin Sin. Anisotropic plasma with a chemical potential and scheme-independent instabilities. *Phys. Lett. B*, 734:116–121, 2014.
- [51] Elliot Banks and Jerome P. Gauntlett. A new phase for the anisotropic N=4 super Yang-Mills plasma. *JHEP*, 09:126, 2015.
- [52] Daniel Ávila, Daniel Fernández, Leonardo Patiño, and Diego Trancanelli. Thermodynamics of anisotropic branes. *JHEP*, 11:132, 2016.
- [53] Dimitrios Giataganas, Umut Gürsoy, and Juan F. Pedraza. Strongly-coupled anisotropic gauge theories and holography. *Phys. Rev. Lett.*, 121(12):121601, 2018.
- [54] Georgios Itsios, Niko Jokela, Jarkko Järvelä, and Alfonso V. Ramallo. Low-energy modes in anisotropic holographic fluids. *Nucl. Phys. B*, 940:264–291, 2019.
- [55] Si-wen Li, Sen-kai Luo, and Hao-qian Li. Holographic Schwinger effect and electric instability with anisotropy. *JHEP*, 08:206, 2022.
- [56] Eric D’Hoker and Per Kraus. Magnetic Brane Solutions in AdS. *JHEP*, 10:088, 2009.
- [57] David Dudal and Thomas G. Mertens. Melting of charmonium in a magnetic field from an effective AdS/QCD model. *Phys. Rev. D*, 91:086002, 2015.
- [58] Kiminad A. Mamo. Inverse magnetic catalysis in holographic models of QCD. *JHEP*, 05:121, 2015.
- [59] Danning Li, Mei Huang, Yi Yang, and Pei-Hung Yuan. Inverse Magnetic Catalysis in the Soft-Wall Model of AdS/QCD. *JHEP*, 02:030, 2017.
- [60] Romulo Rougemont. Jet quenching parameters in strongly coupled anisotropic plasmas in the presence of magnetic fields. *Phys. Rev. D*, 102(3):034009, 2020.
- [61] Zi-qiang Zhang, Ke Ma, and De-fu Hou. Drag force in strongly coupled supersymmetric Yang–Mills plasma in

- a magnetic field. *J. Phys. G*, 45(2):025003, 2018.
- [62] Jared Reiten and Andrey V. Sadofyev. Drag force to all orders in gradients. *JHEP*, 07:146, 2020.
- [63] Zi-qiang Zhang and Ke Ma. The effect of magnetic field on jet quenching parameter. *Eur. Phys. J. C*, 78(7):532, 2018.
- [64] Krishna Rajagopal and Andrey V. Sadofyev. Chiral drag force. *JHEP*, 10:018, 2015.
- [65] Zi-qiang Zhang. Light quark energy loss in strongly coupled $\mathcal{N} = 4$ SYM plasma with magnetic field. *Phys. Lett. B*, 793:308–312, 2019.
- [66] Stefano Ivo Finazzo, Renato Critelli, Romulo Rougemont, and Jorge Noronha. Momentum transport in strongly coupled anisotropic plasmas in the presence of strong magnetic fields. *Phys. Rev. D*, 94(5):054020, 2016. [Erratum: *Phys.Rev.D* 96, 019903 (2017)].
- [67] Oliver DeWolfe, Steven S. Gubser, and Christopher Rosen. A holographic critical point. *Phys. Rev. D*, 83:086005, Apr 2011.
- [68] Oliver DeWolfe, Steven S. Gubser, and Christopher Rosen. Dynamic critical phenomena at a holographic critical point. *Phys. Rev. D*, 84:126014, Dec 2011.
- [69] U. Gursoy, E. Kiritsis, and F. Nitti. Exploring improved holographic theories for QCD: Part II. *JHEP*, 02:019, 2008.
- [70] Alfonso Ballon-Bayona, Henrique Boschi-Filho, Luis A. H. Mamani, Alex S. Miranda, and Vilson T. Zanchin. Effective holographic models for QCD: glueball spectrum and trace anomaly. *Phys. Rev. D*, 97(4):046001, 2018.
- [71] Song He, Shang-Yu Wu, Yi Yang, and Pei-Hung Yuan. Phase Structure in a Dynamical Soft-Wall Holographic QCD Model. *JHEP*, 04:093, 2013.
- [72] Yi Yang and Pei-Hung Yuan. A Refined Holographic QCD Model and QCD Phase Structure. *JHEP*, 11:149, 2014.
- [73] Umut Gursoy, Matti Järvinen, Giuseppe Policastro, and Natale Zinnato. Analytic long-lived modes in charged critical plasma. *JHEP*, 06:018, 2022.
- [74] Romulo Rougemont, Renato Critelli, and Jorge Noronha. Holographic calculation of the QCD crossover temperature in a magnetic field. *Phys. Rev. D*, 93(4):045013, 2016.
- [75] Hardik Bohra, David Dudal, Ali Hajilou, and Subhash Mahapatra. Anisotropic string tensions and inversely magnetic catalyzed deconfinement from a dynamical AdS/QCD model. *Phys. Lett. B*, 801:135184, 2020.
- [76] Song He, Yi Yang, and Pei-Hung Yuan. Analytic Study of Magnetic Catalysis in Holographic QCD. 4 2020.
- [77] Irina Aref’eva and Kristina Rannu. Holographic Anisotropic Background with Confinement-Deconfinement Phase Transition. *JHEP*, 05:206, 2018.
- [78] Irina Ya. Aref’eva, Kristina Rannu, and Pavel Slepov. Holographic anisotropic model for light quarks with confinement-deconfinement phase transition. *JHEP*, 06:090, 2021.
- [79] Meng-Wei Li, Yi Yang, and Pei-Hung Yuan. Approaching Confinement Structure for Light Quarks in a Holographic Soft Wall QCD Model. *Phys. Rev. D*, 96(6):066013, 2017.
- [80] PS Slepov. A way to improve the string tension dependence on temperature in holographic model. *Physics of Particles and Nuclei*, 52(4):560–563, 2021.
- [81] Shanshan Cao and Steffen A. Bass. Thermalization of charm quarks in infinite and finite QGP matter. *Phys. Rev. C*, 84:064902, 2011.
- [82] Guy D. Moore and Derek Teaney. How much do heavy quarks thermalize in a heavy ion collision? *Phys. Rev. C*, 71:064904, 2005.
- [83] Zhou-Run Zhu, Sheng-Qin Feng, Ya-Fei Shi, and Yang Zhong. Energy loss of heavy and light quarks in holographic magnetized background. *Phys. Rev. D*, 99(12):126001, 2019.
- [84] Zhou-Run Zhu, Jun-Xia Chen, Xian-Ming Liu, and Defu Hou. Thermodynamics and energy loss in D dimensions from holographic QCD model. 9 2021.
- [85] Umut Gursoy, Elias Kiritsis, Liuba Mazzanti, and Francesco Nitti. Langevin diffusion of heavy quarks in non-conformal holographic backgrounds. *JHEP*, 12:088, 2010.
- [86] Dimitrios Giataganas. Probing strongly coupled anisotropic plasma. *JHEP*, 07:031, 2012.